

Czech Technical University in Prague  
Faculty of Nuclear Sciences and Physical Engineering  
Department of Physics

*Vector meson electro-production within the  
energy-dependent hot-spot model*

**Jan Cepila**

based on

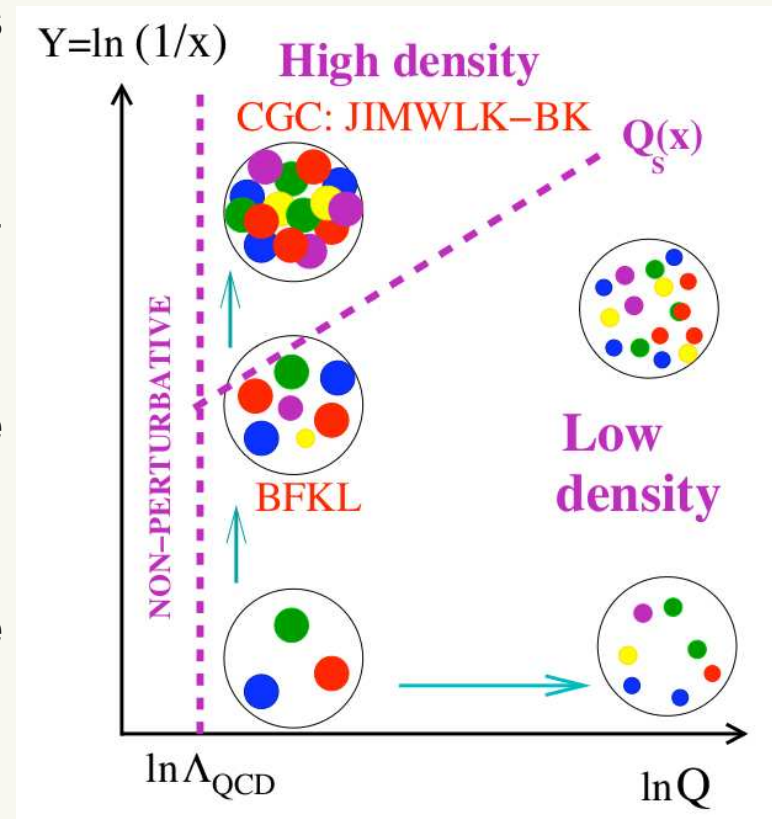
J. Cepila, J.G. Contreras, D.T. Takaki, Phys.Lett. B766 (2017) 186-191

J. Cepila, J.G. Contreras, M. Krelina, Phys.Rev. C97 (2018) no.2, 024901

J. Cepila, J.G. Contreras, M. Krelina, D.T. Takaki, Nucl.Phys. B934 (2018) 330-340

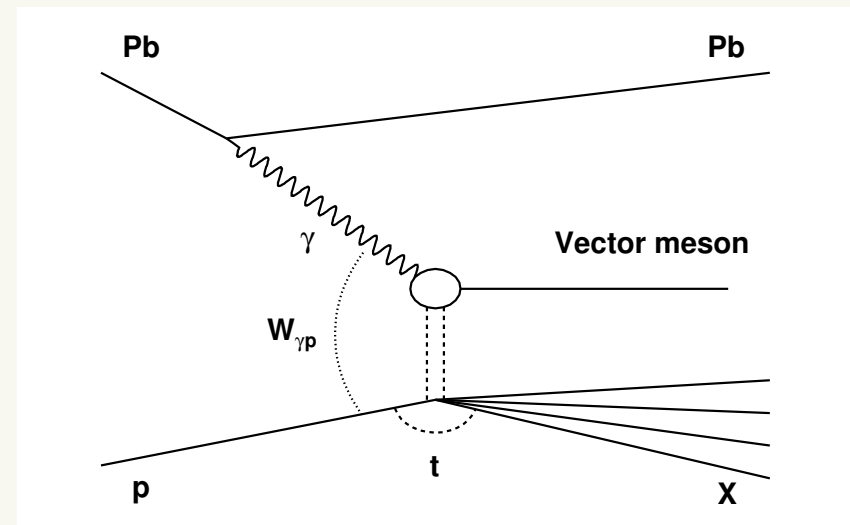
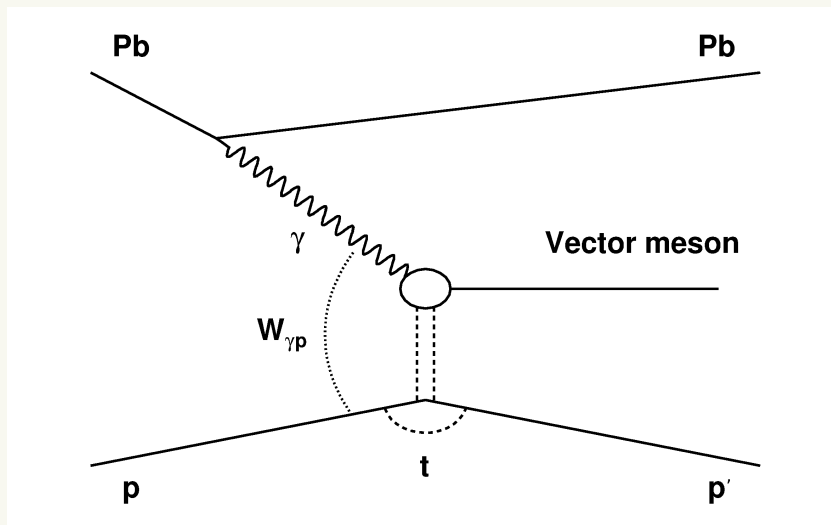
# Gluon saturation

- Exclusive and dissociative vector meson production can be an excellent probe to the gluon structure of the target
  - The vector meson mass and photon scale fixes the position in  $\ln Q^2$
  - Moving to smaller  $x$  one can reach and go beyond the saturation scale  $Q_s(x)$
  - Linear evolution of the gluon density below the saturation scale  $Q_s(x)$  (dilute regime)
  - Non-linear evolution above the saturation scale (dense regime)  $\rightarrow$  gluon saturation
- 
- We show that including geometrical fluctuations a signal of saturation can be seen in the energy dependence of dissociative vector meson production off protons and nuclei at LHC energies.



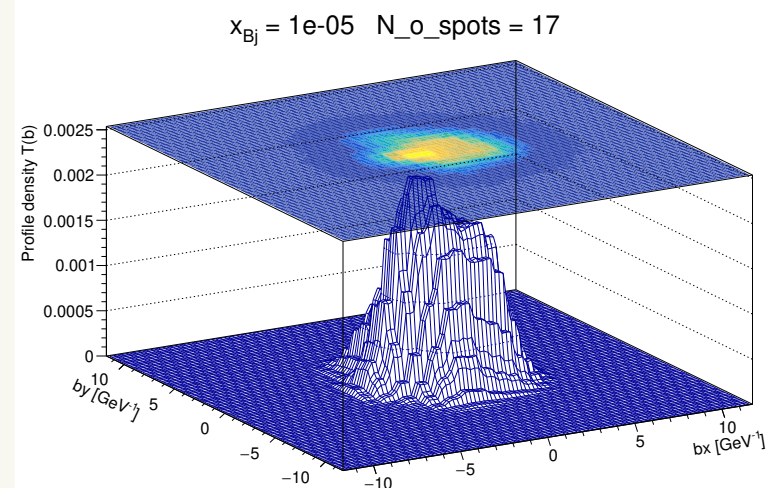
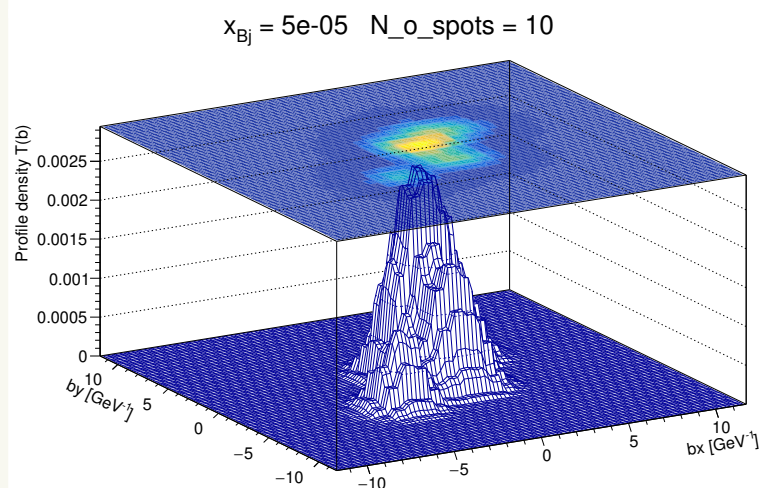
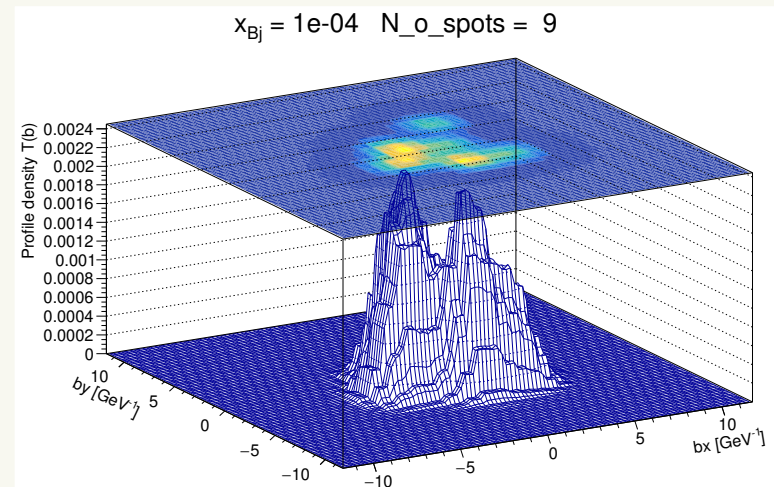
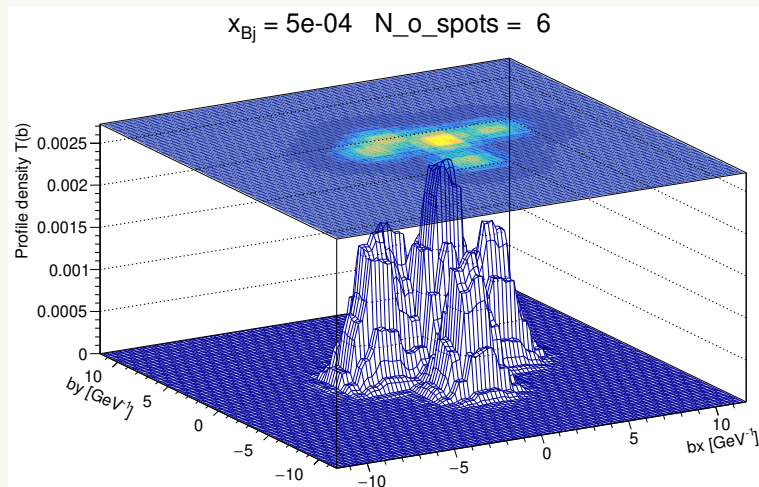
# Kinematics

- The Mandelstam variable  $t = (p' - p)^2$  is the square of the four-momentum transferred at the proton vertex
  - $W_{\gamma p}$  is the center-of-mass energy of the photon-proton system
  - Bjorken- $x$  of the produced meson is
$$x_{Bj} = \frac{M_V^2 + Q^2}{W_{\gamma p}^2 + Q^2}$$
- $M_V$  is the mass of the vector meson,  $Q^2$  is the scale of the incoming photon
- Low- $x$  limit (saturation regime) manifests at large  $W_{\gamma p}$



# Fluctuations

- Exclusive cross section = average over many geometrical configurations
- Dissociative cross section = variance over many geometrical configurations
- Configurations are represented by hot spots positions - number grows with energy



# Production of vector mesons off proton in the color dipole model

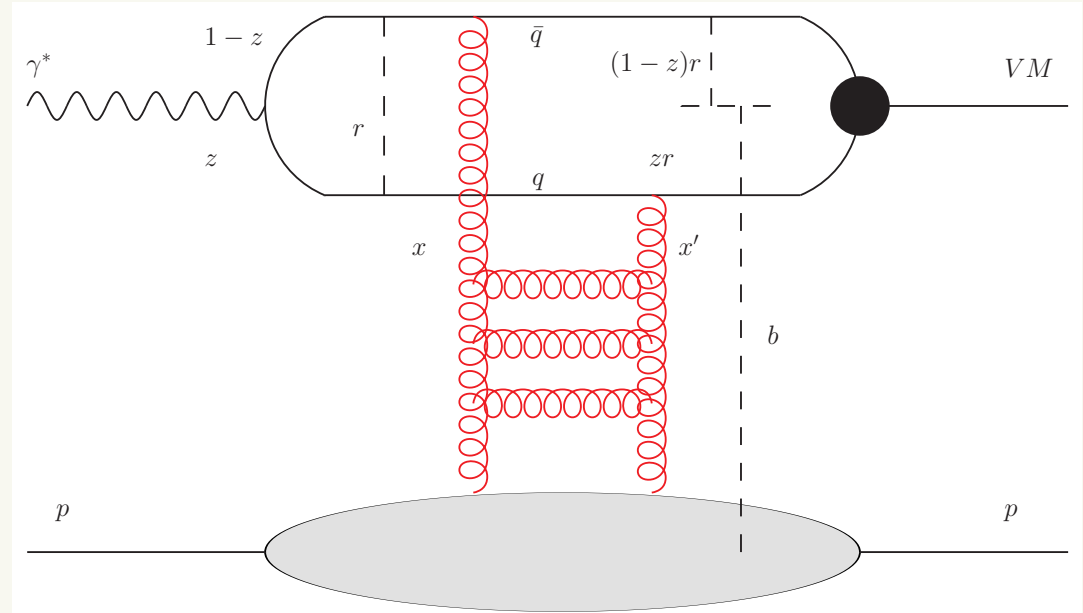
- In the rest frame of the target a photon interacts via its  $q\bar{q}$  Fock component, which collapses into the vector meson

$z$  - fraction of the photon momenta carried by the dipole quark

$r$  - transverse width of the dipole

$b$  - impact parameter of the  $\gamma p$  collision

$$\Delta = \sqrt{-t}$$



- The scattering amplitude is given by the convolution of photon  $\Psi_{\gamma^*}$  and meson  $\Psi_M$  wave functions with the dipole cross section  $d\sigma_{q\bar{q}}/d^2b$

$$\mathcal{A}_{T,L}^{\gamma^* p \rightarrow Mp}(x, Q, \Delta) = i \int d^2r \int_0^1 \frac{dz}{4\pi} \int d^2b \Psi_M^* \Psi_{\gamma^*} \Big|_{T,L} e^{-i(\vec{b} - (1-z)\vec{r})\Delta} \frac{d\sigma_{q\bar{q}}}{d^2b}$$

$T, L$  denote the transverse and longitudinal degrees of freedom of the photon

## Wave function

- Overlap of a virtual photon and vector meson wave function of the  $|q\bar{q}\rangle$  Fock state

$$\Psi_M^* \Psi_{\gamma^*} \Big|_T = e_f \delta_{f\bar{f}} e \frac{N_c}{\pi z(1-z)} \left( m_f^2 K_0(\varepsilon r) \Phi_T(r, z) - (z^2 + (1-z)^2) \varepsilon K_1(\varepsilon r) \partial_r \Phi_T(r, z) \right)$$

$$\Psi_M^* \Psi_{\gamma^*} \Big|_L = e_f \delta_{f\bar{f}} e \frac{N_c}{\pi} 2Qz(1-z) K_0(\varepsilon r) \left( M_V \Phi_L(r, z) + \delta \frac{m_f^2 - \nabla_r^2}{M_V z(1-z)} \Phi_L(r, z) \right)$$

$$\Phi_{T,L}(r, z) = N_{T,L} z(1-z) e^{-\frac{m_f^2 R^2}{8z(1-z)} - \frac{2z(1-z)r^2}{R^2} + \frac{m_f^2 R^2}{2}}$$

$$\varepsilon^2 = z(1-z)^2 Q^2 + m_f^2$$

- The vector meson wave function is calculated with the presumption that the vector meson is predominantly a quark-antiquark state and the spin and polarization structure is the same as in the photon case.
- boosted Gaussian model of the scalar part  $\Phi_{T,L}$  - the  $q\bar{q}$  dipole wave function in the rest frame is modeled with a Gaussian shape and boosted to the proper frame

K.Golec-Biernat and M.Wusthoff, Phys. Rev. D **59**, 014017 (1999); B. E. Cox, J. R. Forshaw, and R. Sandapen, JHEP **06**, 034 (2009)

## Dipole cross section

- From the optical theorem

$$\frac{d\sigma_{q\bar{q}}}{d^2b} = 2N(x, r, b)$$

- Data are integrated over impact parameter - we can access only  $\sigma_{dip}(x, r)$  - impact parameter dependence has to be modeled

$$2N(x, r, b) = \sigma_0 N(x, r) T(b)$$

- $\sigma_0 = 4\pi B_p$  is a model dependent normalization
- $N(x, r)$  is the dipole scattering amplitude of a dipole with transverse size  $r$
- $T(b)$  is the transverse profile of a proton
- Golec-Biernat and Wusthoff model

$$N(x, r) = \left(1 - e^{-r^2 Q_s^2(x)/4}\right) \quad Q_s^2(x) = Q_0^2(x) \left(\frac{x_0}{x}\right)^\lambda$$

K.J. Golec-Biernat, M. Wusthoff, Phys. Rev. D 59 (1998) 014017, arXiv:hep-ph/9807513

## Dipole cross section

- The transverse profile of the proton is taken as a sum of contributions from randomly sampled areas of high gluon density = hot-spots
- Each hot-spot in the proton is taken as a small Gaussian distribution with the width  $B_{hs} = 0.8\text{GeV}^{-2}$  put in an arbitrary position generated from a 2-D Gaussian distribution centered at (0,0) with the width  $B_p$

$$T_{hs}(\vec{b} - \vec{b}_i) = \frac{1}{2\pi B_{hs}} e^{-\frac{(\vec{b} - \vec{b}_i)^2}{2B_{hs}}}$$

- The number of hot spots is allowed to grow with energy - we take a value from a zero-truncated Poissonian with the mean value

$$N_{hs}(x) = p_0 x^{p_1} (1 + p_2 \sqrt{x}) \quad p_0 = 0.011 \quad p_1 = -0.58 \quad p_2 = 300$$

- The final gluon profile is

$$T(\vec{b}) = \frac{1}{N_{hs}(x)} \sum_{i=1}^{N_{hs}(x)} T_{hs}(\vec{b} - \vec{b}_i)$$



## Vector mesons off proton in the color dipole model

- Skewedness correction - gluons attached to quarks in the  $q\bar{q}$  dipole carry different light-front momenta fractions  $x$  and  $x'$  of the proton - the skewness effect

$$R_g^{T,L}(\lambda) = \frac{2^{2\lambda^{T,L}+3} \Gamma(\lambda^{T,L} + 5/2)}{\sqrt{\pi} \Gamma(\lambda^{T,L} + 4)} \quad \lambda^{T,L} = \frac{\partial \ln \mathcal{A}_{T,L}^{\gamma^* p \rightarrow Mp}}{\partial \ln \frac{1}{x}}$$

A.G. Shuvaev, K.J. Golec-Biernat, A.D. Martin, M.G. Ryskin, Phys. Rev. D 60 (1999) 014015

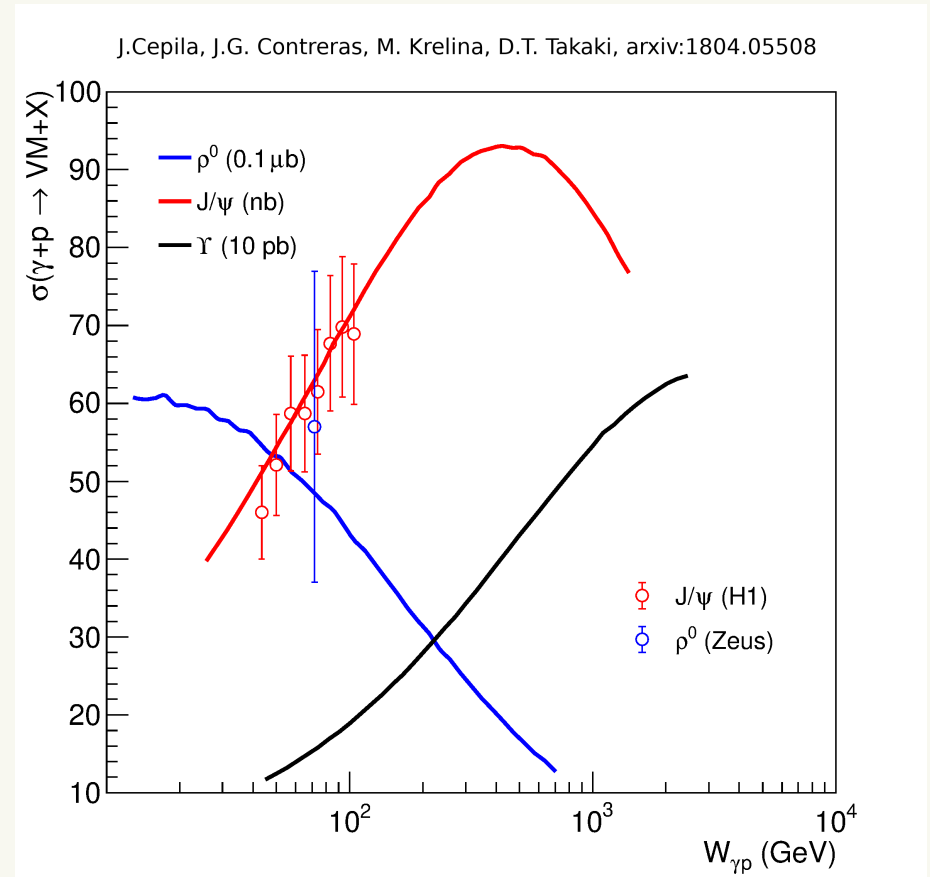
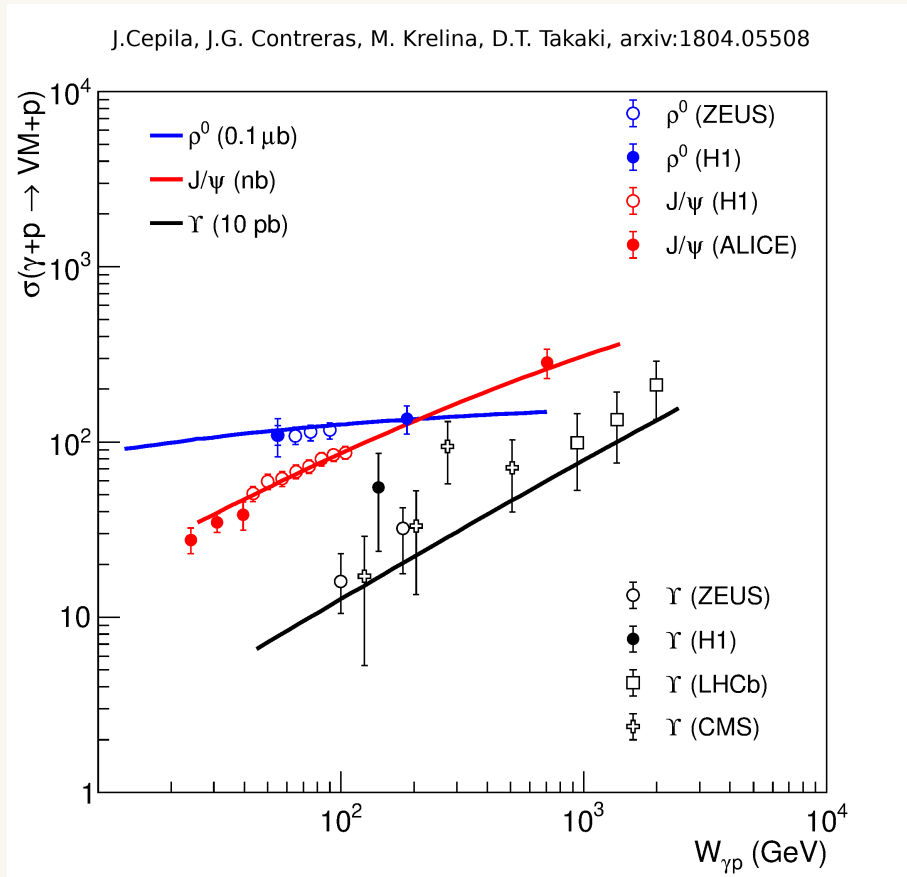
- Final formula for exclusive production is

$$\frac{d\sigma_{T,L}^{\gamma^* p \rightarrow Mp}}{d|t|} = \frac{1}{16\pi} \left| \left\langle \mathcal{A}_{T,L}^{\gamma^* p \rightarrow Mp} R_g^{T,L} \right\rangle \right|^2$$

- Final formula for dissociative production is

$$\frac{d\sigma_{T,L}^{\gamma^* p \rightarrow MX}}{d|t|} = \frac{1}{16\pi} \left( \left\langle \left| \mathcal{A}_{T,L}^{\gamma^* p \rightarrow Mp} R_g^{T,L} \right|^2 \right\rangle - \left| \left\langle \mathcal{A}_{T,L}^{\gamma^* p \rightarrow Mp} R_g^{T,L} \right\rangle \right|^2 \right)$$

# Exclusive and dissociative $\rho$ , $J/\psi$ and $\Upsilon$ photo-production off protons



## Modification of the model for nuclear targets

- Glauber-Gribov (GG) approach

$$\left( \frac{d\sigma_{q\bar{q}}^A}{d^2b} \right)_j = 2 \left( 1 - e^{-\frac{1}{2}\sigma_{q\bar{q}}(x,r)T_A^j(\vec{b})} \right)$$

Position of nucleons is chosen randomly from the Woods-Saxon distribution

- Geometric scaling inspired (GS) approach

$$\left( \frac{d\sigma_{q\bar{q}}^A}{d^2b} \right)_j = \sigma_0^A N^A(x,r) T_A^j(\vec{b})$$

$$N^A(x,r) = \left( 1 - e^{-\frac{r^2 Q_{sA}^2(x)}{4}} \right) \quad Q_{sA}^2(x) = Q_s^2(x) \left( \frac{A\pi R_p^2}{\pi R_A^2} \right)^{\frac{1}{\delta}} \quad \sigma_0^A = \pi R_A^2$$

N. Armesto, C. A. Salgado, U. A. Wiedemann, Phys. Rev. Lett. 94 (2005) 022002, arXiv:hep-ph/0407018

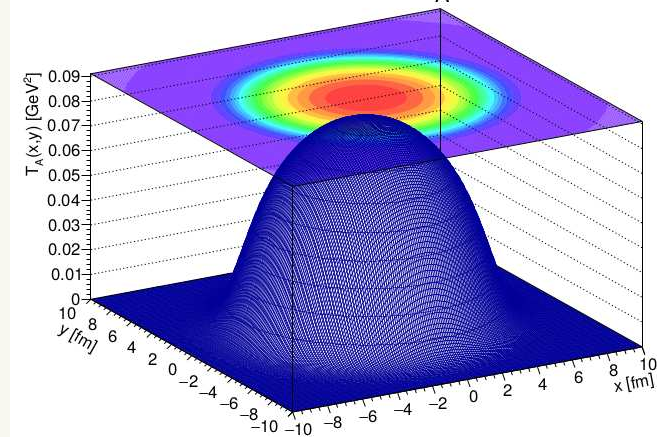
$R_A$  is the nuclear radius from Woods-Saxon distribution,  $R_p = \sqrt{2B_p}$  is the proton radius,  $\delta = 0.8$

# Modification of the model for nuclear targets

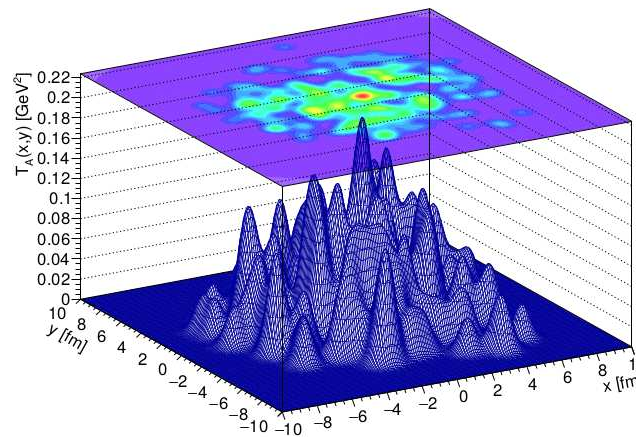
Two variants of the transverse profile

- Fluctuations in nucleon positions only (GG-n, GS-n)
- Fluctuations in nucleon positions and also at a hot-spot level (GG-hs, GS-hs)

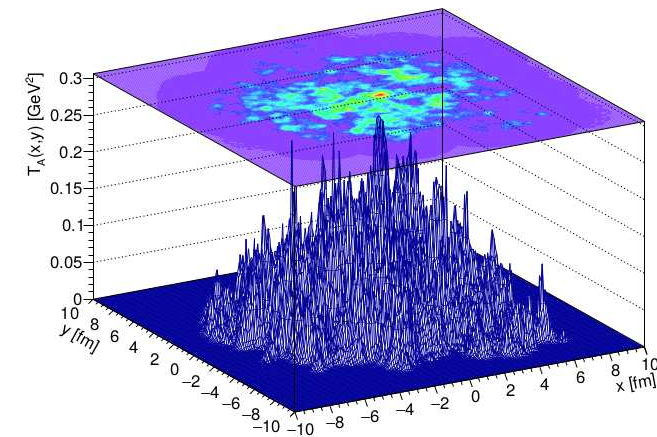
Averaged from  $\rho_A(x,y,z)$



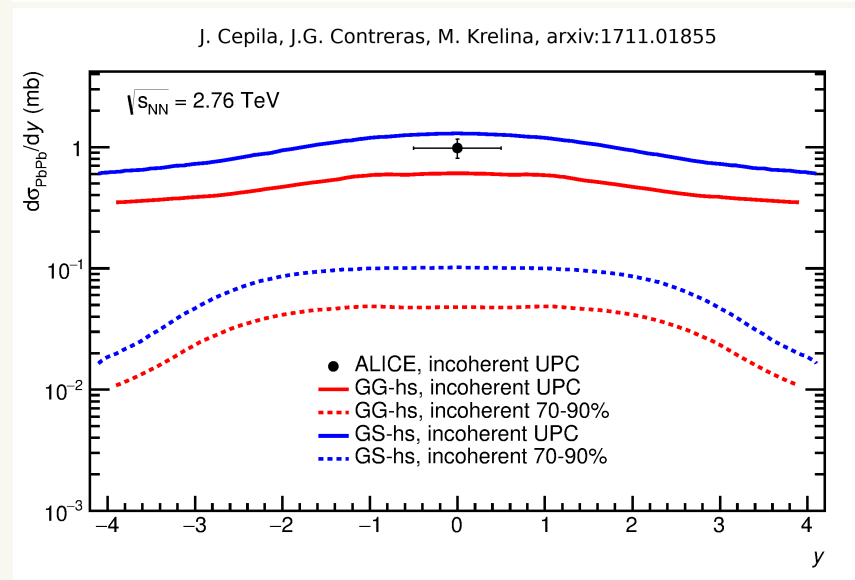
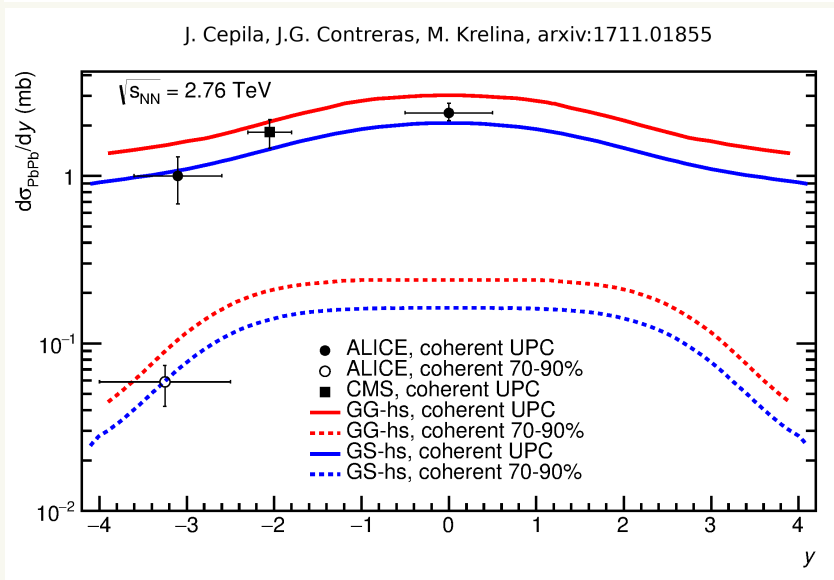
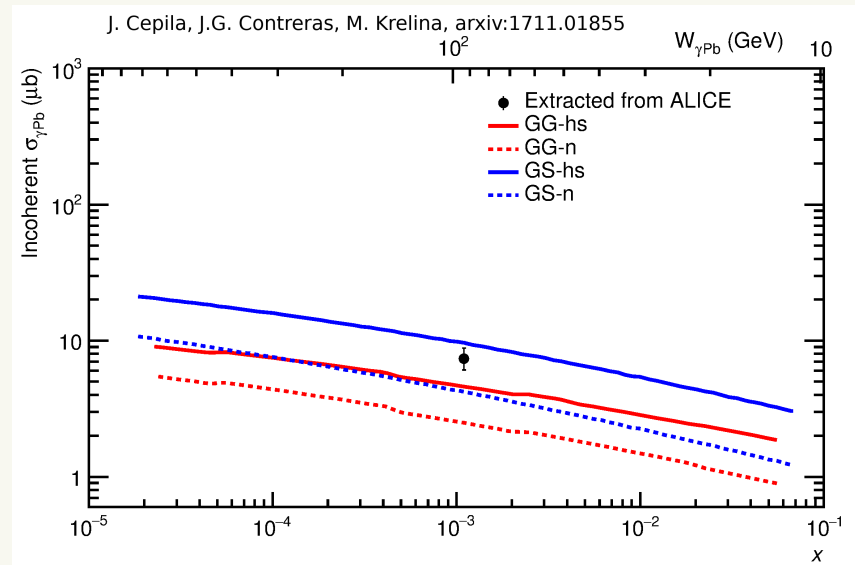
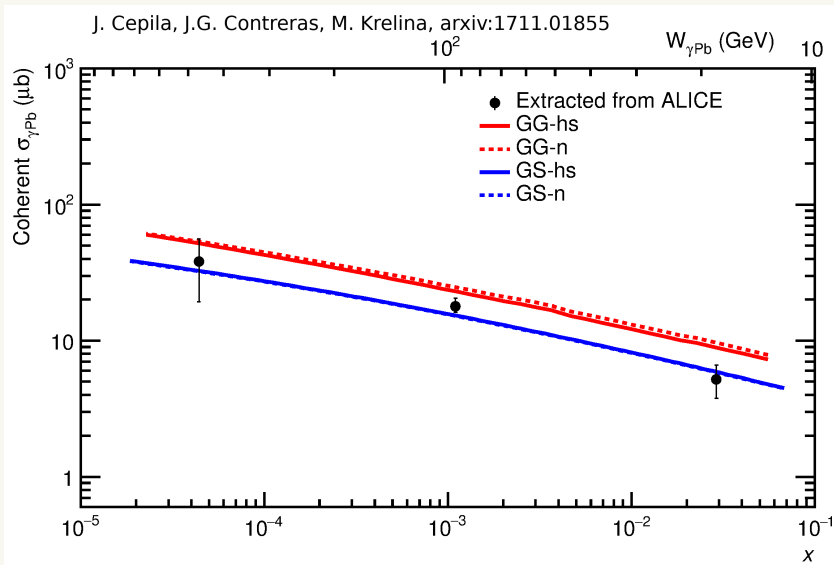
Nucleons configuration



Hot spots configuration



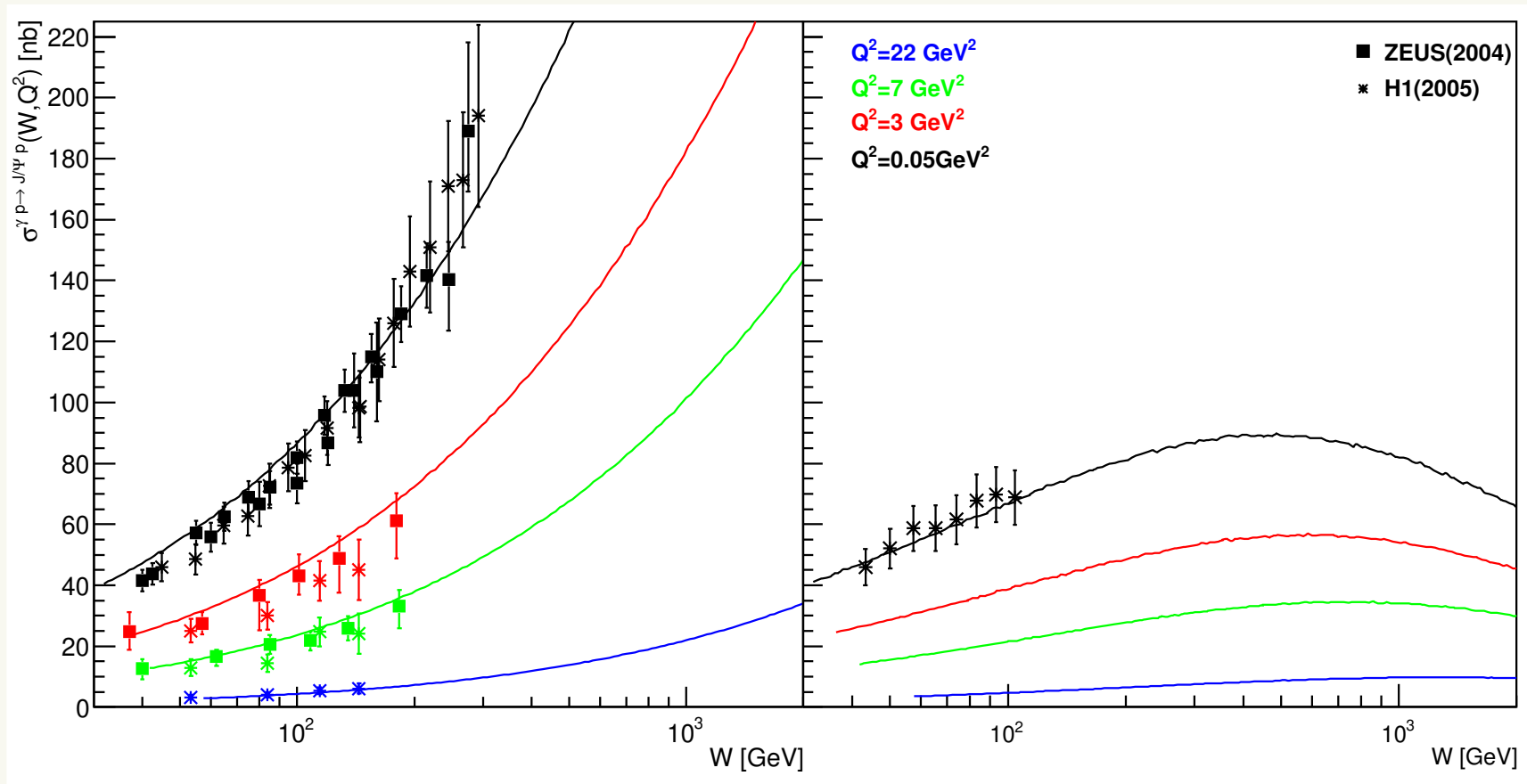
# Coherent and incoherent $J/\psi$ photo-production off nuclei



# Exclusive and dissociative $J/\psi$ electro-production off proton

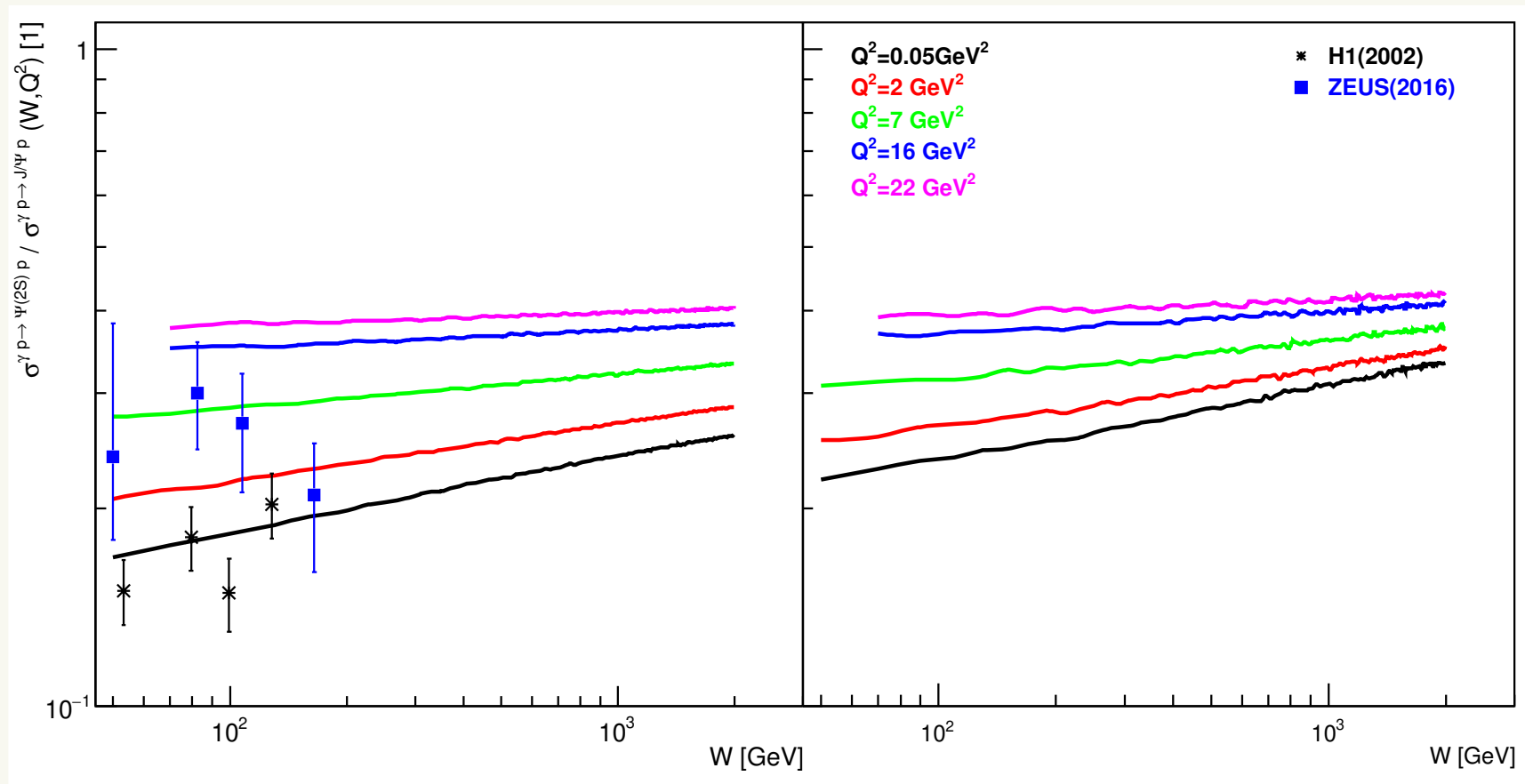
New results for  $J/\psi$  electro-production - parameters are the same as in the case of photo-production

Dissociative maximum moves to higher  $W$  with increasing scale



# Exclusive and dissociative $\psi(2S)/J/\psi$ electro-production off proton

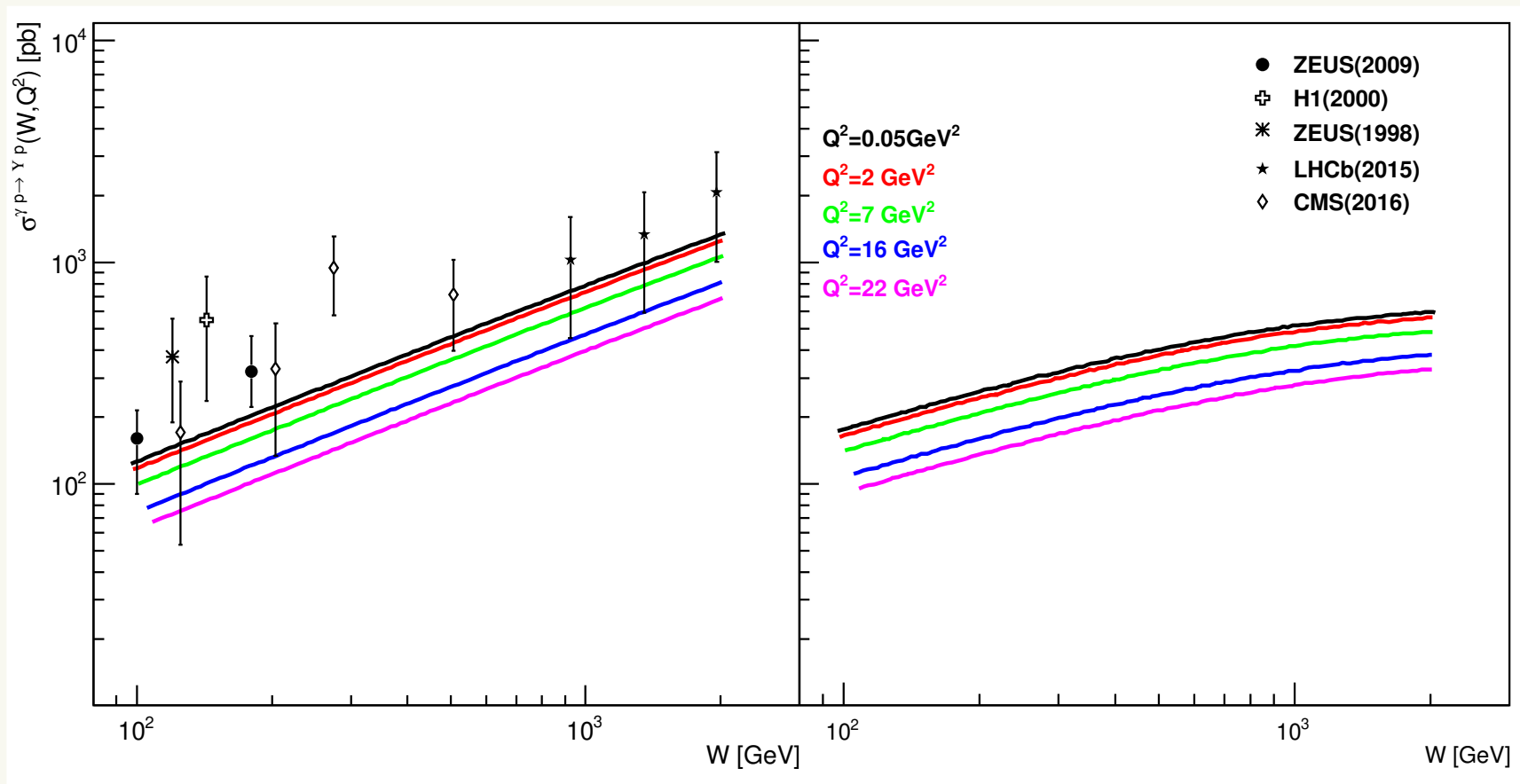
New results for  $\psi(2S)/J/\psi$  electro-production - parameters are the same as in the case of photo-production



# Exclusive and dissociative $\Upsilon$ electro-production off proton

New results for  $\Upsilon$  electro-production - parameters are the same as in the case of photo-production

Dissociative maximum moves to higher  $W$  with increasing scale very slowly

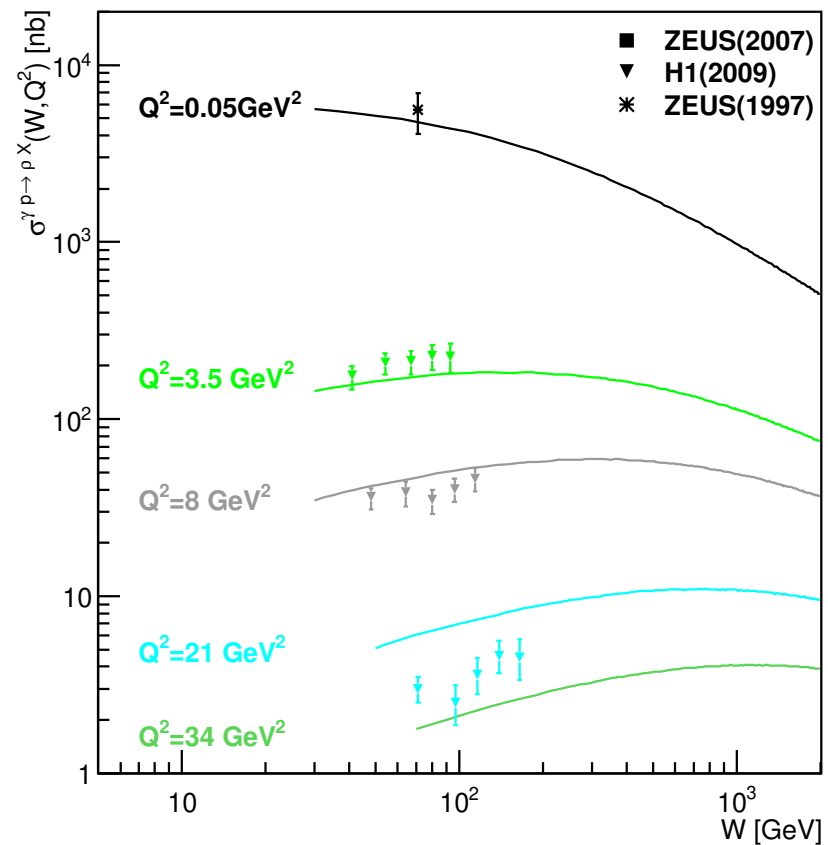
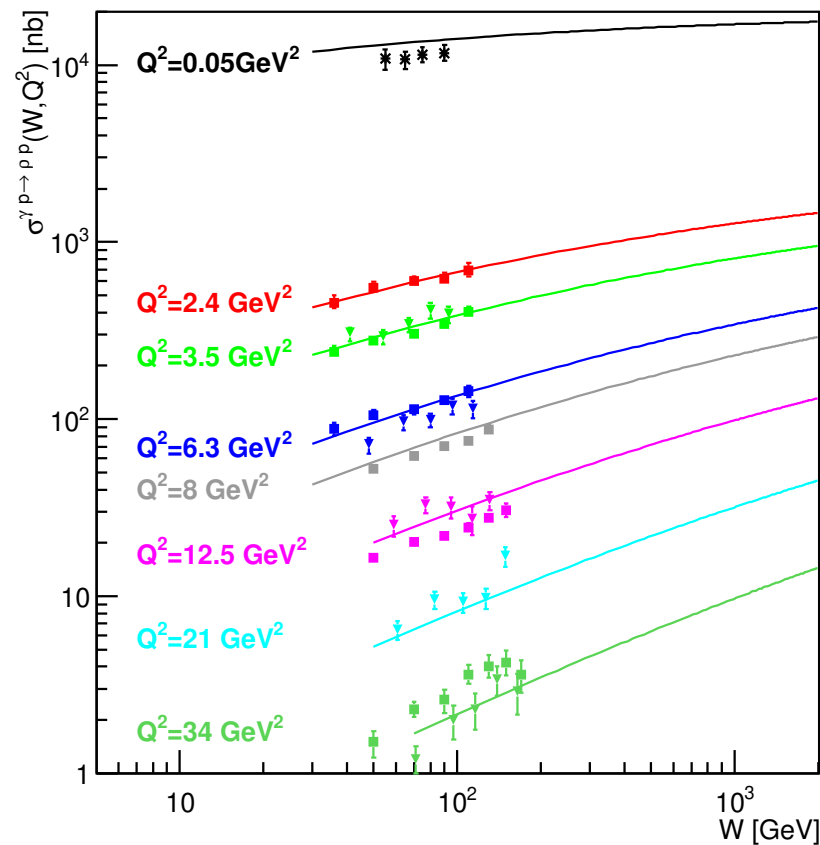




# Exclusive and dissociative $\rho$ electro-production off proton

New results for  $\rho$  electro-production -  $B_p$  has to be changed for low mass vector mesons according to HERA measurements of the slope parameter to  $B_p = 8\text{GeV}^{-2}$  at  $Q^2 = 0$  while  $B_p = 4.7\text{GeV}^{-2}$  at  $Q^2 > 0$

Dissociative maximum moves very strongly with increasing scale

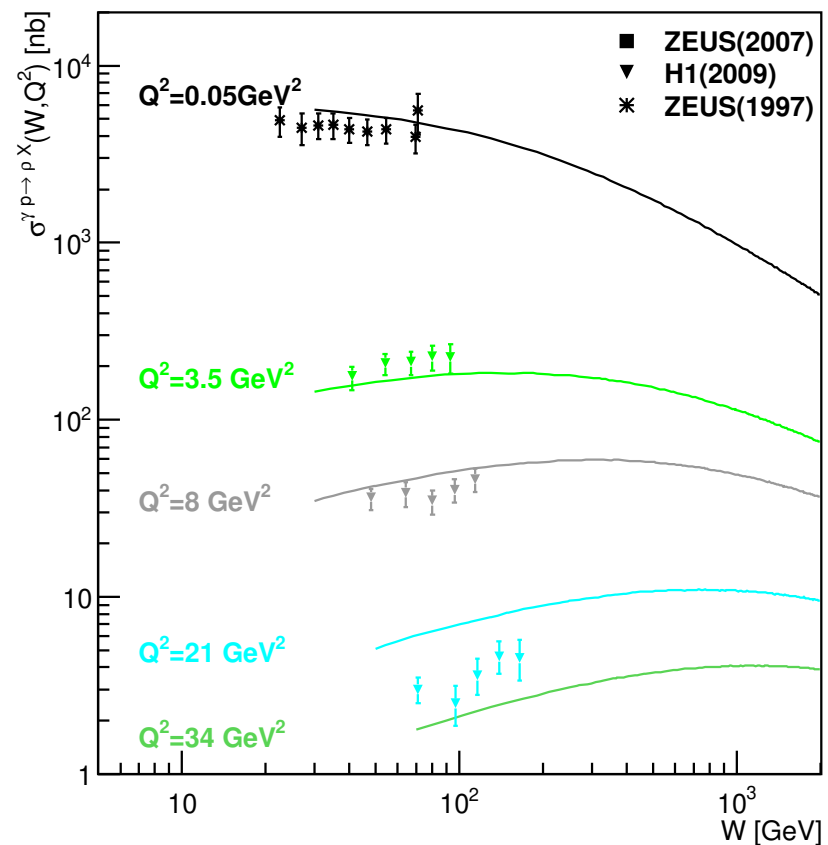
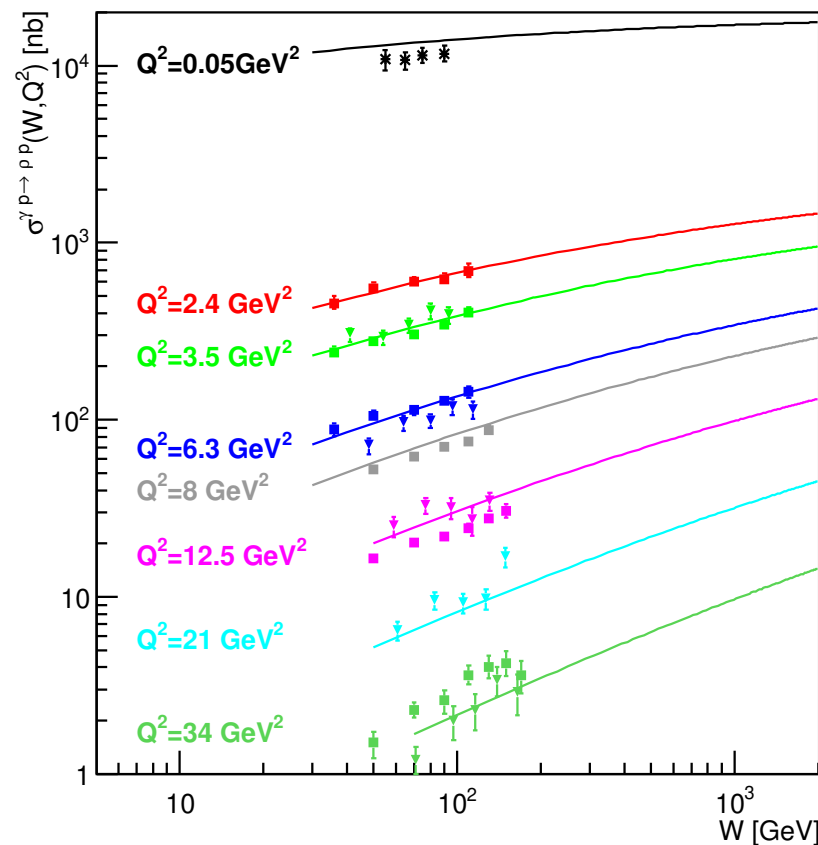


# Exclusive and dissociative $\rho$ electro-production off proton

New results for  $\rho$  electro-production -  $B_p$  has to be changed for low mass vector mesons according to HERA measurements of the slope parameter to  $B_p = 8\text{GeV}^{-2}$  at  $Q^2 = 0$  while  $B_p = 4.7\text{GeV}^{-2}$  at  $Q^2 > 0$

Dissociative maximum moves very strongly with increasing scale

Including H1 preliminary data from ICHEP 2018



## Discussion

The numerical values were chosen according to the following arguments:

- The average square of the proton radius  $B_p = 4.7\text{GeV}^{-2}$  is similar to that measured at HERA, rise of  $B_p$  for  $\rho$  meson is motivated by the rise of the slope parameter for small masses and scales also seen at HERA.  $B_p(W)$  according to H1 measurement for  $J/\psi$  can be used - induces change of parameters in  $N_{hs}(x)$ .
- The value of the average square of the hot spot radius  $B_{hs} = 0.8\text{GeV}^{-2}$  corresponds to a hot spot radius of 0.35 fm, quite close to the values around 0.3 fm found in several papers on soft QCD structure
- The value of  $\lambda = 0.21$  is constrained by the energy dependence of exclusive  $J/\Psi$  photo-production, similar to the value found at HERA for a scale  $Q^2 \sim 2-3\text{GeV}^2$
- Due to the factorized form of the dipole cross section we can set  $\sigma_0 = 4\pi B_p$ .
- We related the number of hot spots with the number of gluons available for the interaction - we follow a simple functional form for the gluon distribution with coefficients varied to find best agreement with the energy dependence of H1 data of exclusive  $J/\Psi$  photo-production
- Results for electro-production and for nuclear targets calculated without any additional parameter.

## Main results

- The model predicts that the energy dependence of the dissociative process increases from low energies up to  $W_{\gamma p} \sim 500$  GeV for  $J/\psi$  and then decreases steeply - this energy range can be explored at HERA and LHC.
- The physics explanation according to the parton saturation phenomenon is that the growth of the number of scattering centers provides the growth of the exclusive and dissociative cross section. However, at some point the number of hot spots is so large that they overlap. When the overlap is large enough, different configurations look the same and the variance diminishes and so does the dissociative cross section.
- Photo-production of  $\rho$  and  $\Upsilon$  as well as electro-production of vector mesons on a proton target within the energy-dependent hot-spot model provides a mass and a scale dependence of the saturation signal. It gives a new handle in the search for saturation effects - this can be checked experimentally by re-processing data from HERA.
- Fluctuations of subnuclear degrees of freedom also leave an imprint in the photo-production of  $J/\psi$  off nuclear targets. The energy dependence on the number of the subnuclear degrees of freedom produces and energy dependence on the ratio of incoherent to coherent cross section.

Backup slides

## DIS within the same framework

- We did a test of the model prediction for DIS, also - see result compared to data at  $Q^2 = 2.7\text{GeV}^2$

$$F_2(x, Q^2) = \frac{Q^2}{4\pi^2\alpha_{em}} \left( \sigma_T^{\gamma^*p}(x, Q^2) + \sigma_L^{\gamma^*p}(x, Q^2) \right)$$

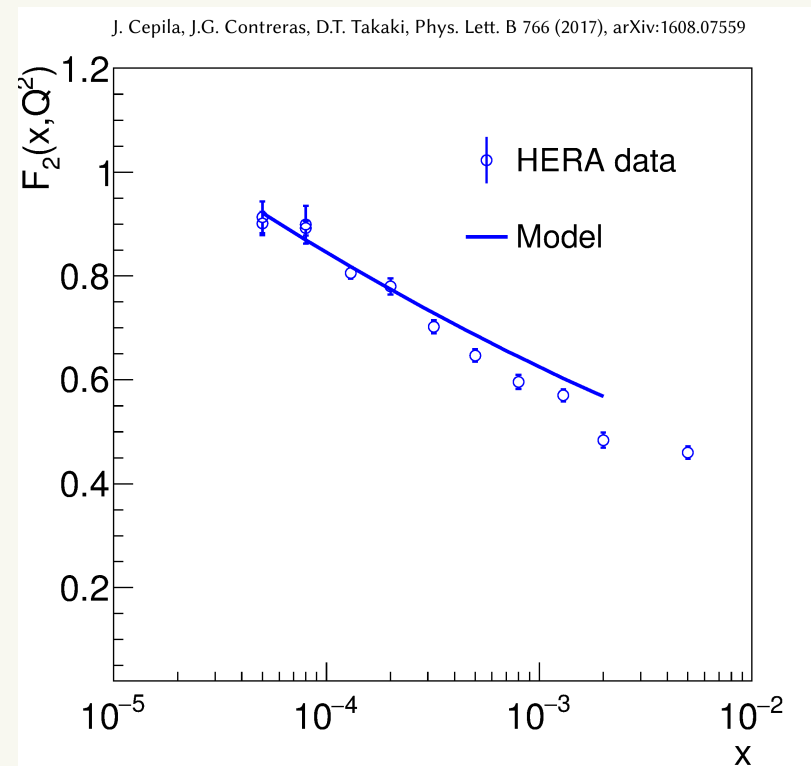
$$\sigma_{T,L}^{\gamma^*p}(x, Q^2) = \sigma_0 \int d\vec{r} \int_0^1 dz |\Psi_{T,L}^{\gamma^* \rightarrow q\bar{q}}(z, r, Q^2)|^2 N(r, \tilde{x})$$

- Parameters are the same as in the vector meson case

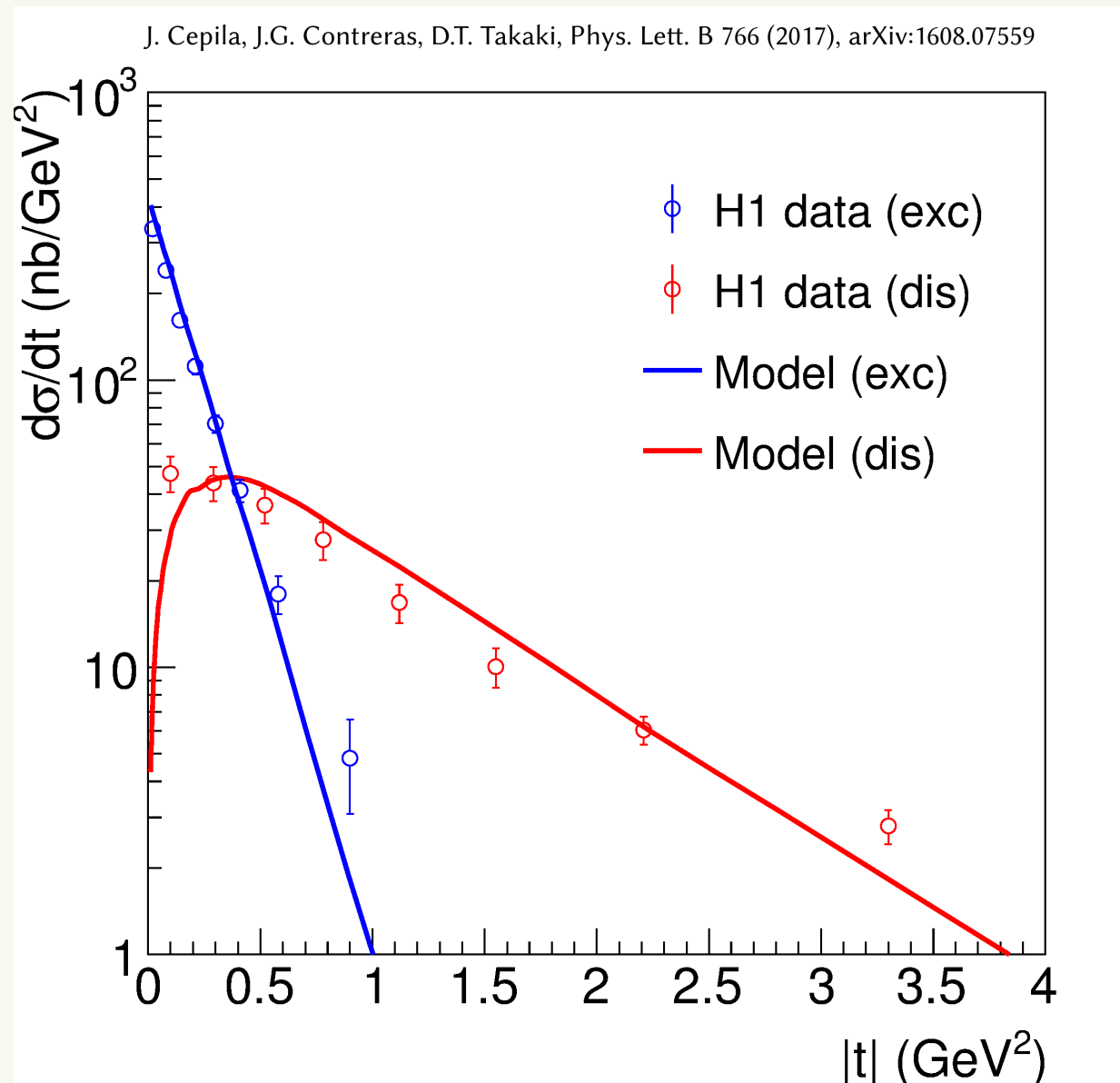
- $\tilde{x} = x(1 + (4m_f^2)/Q^2)$

K.Golec-Biernat and M.Wusthoff, Phys. Rev. D **59**, 014017 (1999)

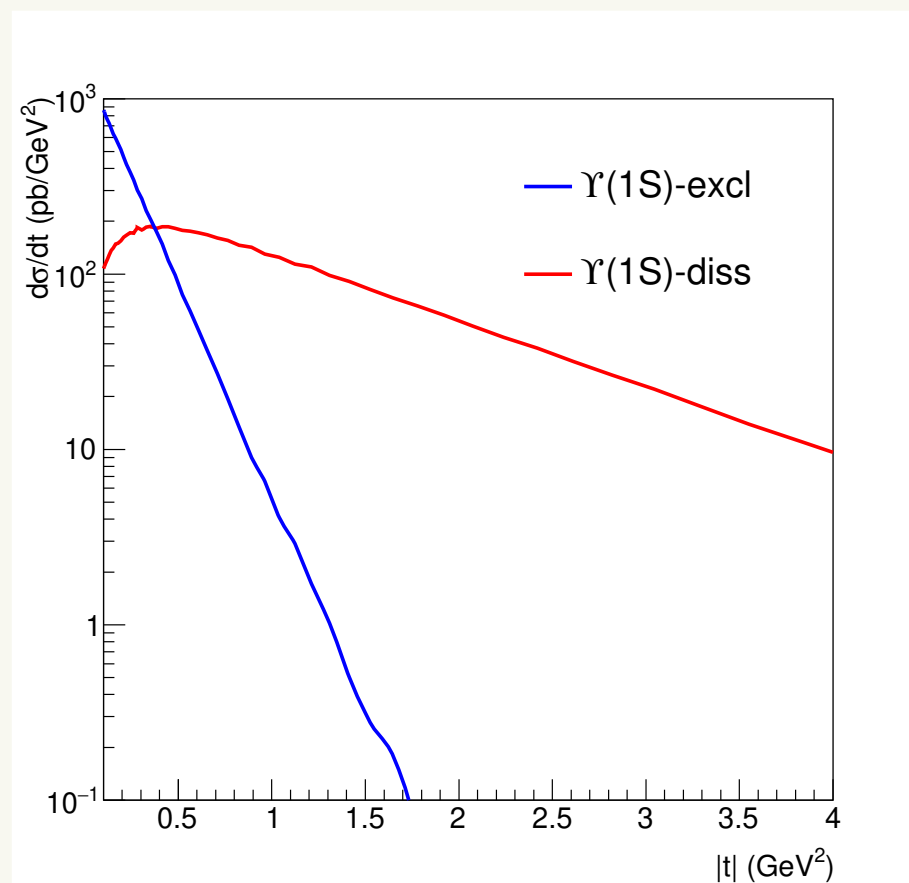
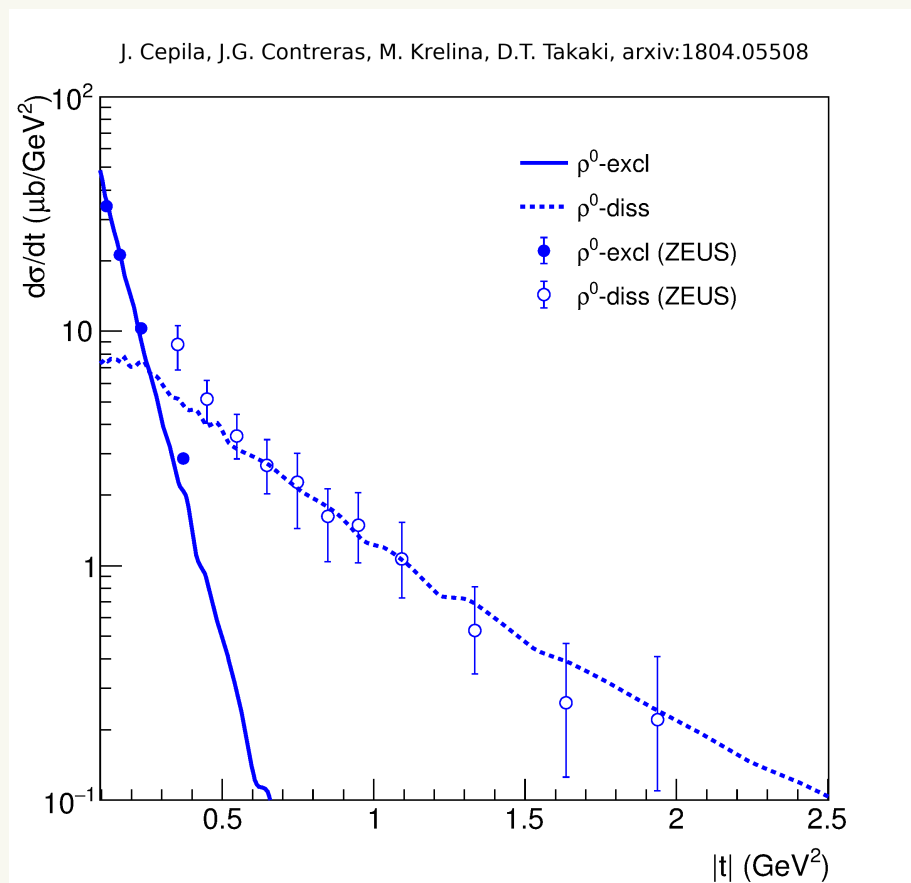
- $N(r, \tilde{x})$  taken from the GBW model
- $m_f$  is an effective mass of a quark



# Exclusive and dissociative t-distribution of $J/\psi$ photo-production off protons



# Exclusive and dissociative t-distribution of $\rho$ and $\Upsilon$ photo-production off protons





# Ratio of coherent to incoherent $J/\psi$ photo-production off nuclei

